

# Nanoscale

Accepted Manuscript



This is an *Accepted Manuscript*, which has been through the Royal Society of Chemistry peer review process and has been accepted for publication.

*Accepted Manuscripts* are published online shortly after acceptance, before technical editing, formatting and proof reading. Using this free service, authors can make their results available to the community, in citable form, before we publish the edited article. We will replace this *Accepted Manuscript* with the edited and formatted *Advance Article* as soon as it is available.

You can find more information about *Accepted Manuscripts* in the [Information for Authors](#).

Please note that technical editing may introduce minor changes to the text and/or graphics, which may alter content. The journal's standard [Terms & Conditions](#) and the [Ethical guidelines](#) still apply. In no event shall the Royal Society of Chemistry be held responsible for any errors or omissions in this *Accepted Manuscript* or any consequences arising from the use of any information it contains.

# Spin-induced band modifications of graphene through intercalation of magnetic iron atoms

S. J. Sung<sup>a</sup>, J. W. Yang<sup>a,c</sup>, P. R. Lee<sup>a</sup>, J. G. Kim<sup>a</sup>, M. T. Ryu<sup>a</sup>, H. M. Park<sup>a</sup>, G. Lee<sup>c</sup>, C. C. Hwang<sup>b</sup>, Kwang. S. Kim<sup>c</sup>, J. S. Kim<sup>a</sup>, J. W. Chung<sup>\*a</sup>

Received Xth XXXXXXXXXXXX 20XX, Accepted Xth XXXXXXXXXXXX 20XX

First published on the web Xth XXXXXXXXXXXX 200X

DOI: 10.1039/b000000x

Intercalation of magnetic iron atoms through graphene formed on the SiC(0001) surface is found to induce significant changes in electronic properties of graphene due mainly to the Fe-induced asymmetries in charge as well as spin distribution. From our synchrotron-based photoelectron spectroscopy data together with *ab initio* calculations, we observe that the Fe-induced charge asymmetry results in the formation of a quasi-free-standing bilayer graphene while the spin asymmetry drives multiple spin-split bands. We find that Fe adatoms are best intercalated upon annealing at 600 °C exhibiting split linear  $\pi$ -bands, characteristic of a bilayer graphene, but much diffused. Subsequent changes in the C 1s, Si 2p, and Fe 3p core levels are consistently described in terms of Fe-intercalation. Our calculations together with a spin-dependent tight binding model ascribe the diffused nature of the  $\pi$ -bands to the multiple spin-split bands originated from the spin-injected carbon atoms residing only in the lower graphene layer.

## 1 Introduction

Because of its surpassing properties of effectively massless charge carriers or Dirac fermions, graphene (G) has been considered as a promising candidate for the next generation carbon-based electronics.<sup>1–6</sup> Among several ways of fabricating graphene, epitaxial growth on silicon carbide (SiC)<sup>7,8</sup> has been efficiently adopted to produce a highly crystalline form of graphene,<sup>9</sup> most suitable for device applications. This method, however, has been hampered by the degraded mobility stemming essentially from the buffer layer.<sup>9–11</sup> Recently, an efficient way to eliminate such adverse influence of the buffer layer has been demonstrated by passivating the interface states with intercalation mechanism.<sup>12–17</sup> A variety of atoms such as hydrogen,<sup>12</sup> lithium,<sup>13</sup> gold,<sup>14</sup> oxygen,<sup>15</sup> germanium,<sup>16</sup> and silicon<sup>17</sup> have been reported to intercalate below the buffer layer and decouple it into a purely  $sp^2$  sheet of graphene.

Here we attempt another possibility of intercalating magnetic iron atoms, Fe, to observe not only the decoupling of the buffer layer but also any spin effect from intercalated atoms on the electronic property of graphene as predicted theoretically for the graphene interacting with nearby magnetic insulator showing magnetic proximity effect.<sup>18</sup> The two-dimensional G/Fe system with spin-controlled band modifications, if any, may well be utilized in spintronics as reported on the G/Fe/Ni(111) system.<sup>19–21</sup> The strong magnetic anisotropy reported on the G/Co/Ir(111) system with magnetization only perpendicular to the surface studied by using

imaging techniques such as spin-polarized low energy electron microscopy suggests a role of graphene to manipulate the direction of magnetization of magnetic films.<sup>22</sup> We have thus investigated the intercalation of Fe atoms for a Fe-adsorbed single layer graphene (SLG) formed on the SiC(0001) surface by measuring changes in the linear  $\pi$ -band (or Dirac band) as well as in surface core levels such as C 1s, Si 2p, and Fe 3p upon intercalation with high resolution photoelectron spectroscopy (HRPES) using synchrotron radiations. We have also carried out *ab initio* density functional theory (DFT) calculations for a minimum energy configuration with Fe atoms intercalated and subsequent changes in the linear Dirac bands. Our measurements show that Fe atoms indeed begin to intercalate when heated above annealing temperature  $T_a=300$  °C into the region below the buffer layer. This intercalation reaches the maximum near  $T_a=600$  °C, where we observe two split linear Dirac bands as typically seen from a bilayer graphene, but much diffused. We also find evidence of Fe-intercalation from changes in the surface core levels. Our DFT calculations for both the spin-integrated and spin-polarized Dirac bands fairly well account for the observed split Dirac bands and its diffused nature primarily in terms of the co-existing multiple spin-polarized (majority and minority) bands thermally broadened at room temperature and jammed together near  $\bar{K}$  of the Brillouin zone. The presence of randomly distributed spin-injected carbon atoms in the lower graphene layer may also contribute somewhat to diffuse the Dirac bands.

## 2 Experimental Details

We have obtained our HRPES data for surface core levels at the beamline 8A2 of the Pohang Accelerator Laboratory in Korea using synchrotron photons of energy either 510 eV or 630 eV. The HRPES chamber was equipped with a hemispherical Scienta 100 analyzer with an overall energy resolution less than 100 meV. The valence bands were measured by using an angle-resolved photoemission spectrometer (ARPES) chamber at the 4A2 beamline equipped with a VG-Scienta R4000 analyzer and a high-flux He I source ( $h\nu=21.2$  eV). The background pressure of the chambers was maintained below  $1 \times 10^{-10}$  Torr during the measurements. We have used a Si terminated n-type 6H-SiC(0001) wafer purchased from Cree as a substrate to grow graphene. We have formed SLG on the SiC(0001) surface following the recipe reported earlier.<sup>23,24</sup> The well-characterized evolution of the LEED pattern upon forming SLG on SiC begins with a Si-rich  $3 \times 3$  phase, which develops into a  $\sqrt{3} \times \sqrt{3}$ -R30° phase when annealed at  $T_a=980$  °C as measured by using an optical pyrometer. We continued to anneal the substrate further to obtain a carbon-rich surface with the  $6\sqrt{3} \times 6\sqrt{3}$  phase in situ at  $T_a=1250$  °C. Although there is a subtle but discernible change in the LEED pattern indicating the formation of SLG, we find the most convincing evidence from the presence of linear Dirac band and the characteristic changes in C 1s and Si 2p core level spectra. We have adopted ion gun sputtering to deposit Fe on the SLG and the deposition rate of  $0.2 \text{ \AA}/\text{min}$  was monitored by a quartz oscillator.

We have also carried out total energy calculation by using *ab initio* DFT with a Vienna simulation package (VASP) within the pseudopotentials and a plane wave basis set.<sup>25</sup> A cutoff energy of 420 eV was set for the plane wave basis, and a k mesh of  $9 \times 9 \times 1$  and  $6 \times 6 \times 1$  was used for the  $2 \times 2$  graphene and  $4 \times 4$  graphene, respectively. A dipole correction has been applied to avoid spurious interactions between the dipoles of repeated slabs along the direction normal to the SiC(0001)-graphene interface.<sup>26</sup> The van der Waals density functional theory (vdW-DFT) was also used to include London dispersion interactions between the graphene, buffer layer, and Fe atoms. The optB86b-vdW functional was used for the exchange-correlation energy, and the projector-augmented wave was used for the electron-ion interactions.<sup>27,28</sup> We have adopted the  $2 \times 2$  graphene on the 6H-SiC (0001) surface with a carbon buffer layer below the graphene layer. The supercells consist of three bilayers of Si-C, C buffer layer above the Si terminated SiC(0001) surface, and graphene layer. The atoms in the bottom bilayer (Si and C) were fixed while the bottom C atoms were passivated with H atoms. We fully relaxed the remaining atoms with a force being restricted to be less than  $0.02 \text{ eV/\AA}$ . The slab was separated by a vacuum layer of thickness greater than  $15 \text{ \AA}$ .

## 3 Data and Analysis

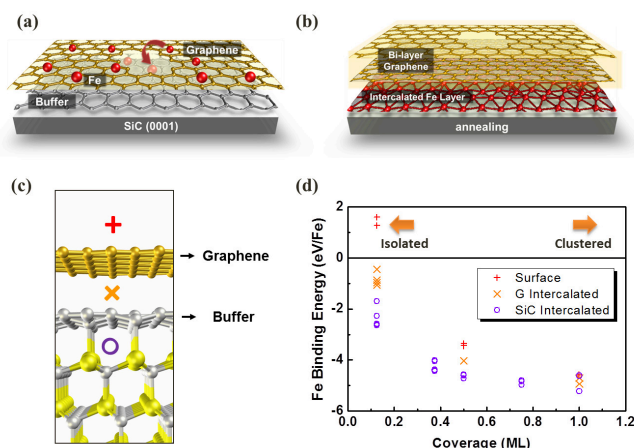


**Fig. 1** (a) Schematic illustration of Fe adsorbed SLG formed on SiC (0001). (b) Possible Fe-intercalation through SLG upon annealing, which decouples the buffer layer to form a bilayer graphene. (c) Three possible locations for intercalated Fe atom; Above (+), below (x) graphene, and below buffer layer (o). (d) Calculated Fe-intercalation energy decreases rapidly with increasing Fe coverage for three intercalation sites, revealing the site below the buffer layer being most stable at all coverage. Note that Fe atoms form a cluster for coverage greater than 0.38 ML.

Figs. 1(a) and (b) schematically illustrate a possible scenario for Fe-intercalation upon annealing the substrate, where Fe may diffuse below SLG through defects or domain boundaries. In order to access the energetics of intercalation for three different intercalation sites depicted in Fig. 1(c), we have examined intercalation energy  $E_{int}$  defined below as a function of Fe coverage for 52 possible different structures.

$$E_{int} = -\frac{1}{N_{Fe}}(E_{tot} - E_{SiC-G} - N_{Fe}E_{Fe}), \quad (1)$$

where  $N_{Fe}$  denotes the number of Fe atoms intercalated, and  $E_{tot}$ ,  $E_{SiC-G}$ , and  $E_{Fe}$  are total energy of the Fe intercalated system, energy of the pristine SiC(0001)-graphene, and energy of an isolated Fe atom, respectively. As shown in Fig. 1(d), Fe atoms are found to intercalate below the buffer layer for all coverages being partially bonded to Si atoms, and decouple the buffer layer into another graphene layer changing the hybridization of carbon atoms from  $sp^3$  into  $sp^2$ . Our HRPES data discussed below strongly support this feature. As shown in Fig. 1(d), the intercalation energy rapidly decreases with increasing Fe coverage for all three intercalation sites, and favors the site below the buffer layer over the other sites for all coverages. It is interesting to note the formation of Fe clusters for coverage greater than 0.38 monolayer (ML) as observed also in our STM images (not shown).

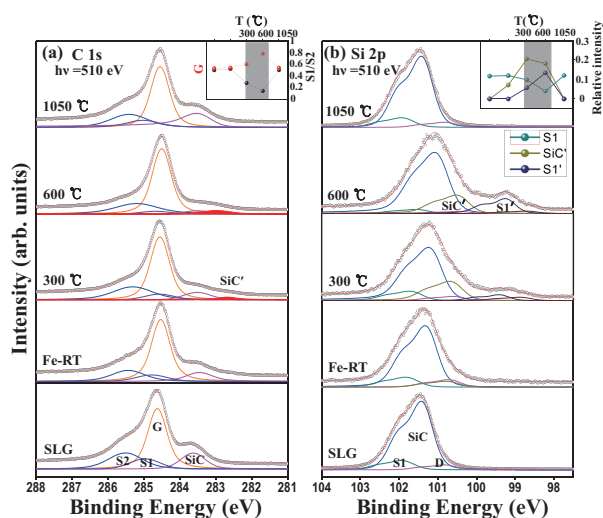


**Fig. 2** Evolution of C 1s (a) and Si 2p (b) core level spectra with increasing  $T_a$  measured by using HRPES with synchrotron photons of energy 510 eV. Inset in (a) shows the change of the normalized intensity G and S1/S2 with increasing  $T_a$ , and inset in (b) shows the corresponding changes of the three newly developed components for Si 2p. The shaded area indicates the region where Fe-intercalation occurs.

The progressive changes in the C 1s and Si 2p core level spectra with increasing  $T_a$  are presented in Fig. 2 measured with synchrotron photons of energy 510 eV. Using a fitting scheme,<sup>10,29,30</sup> we find four components for the C 1s peak denoted as SiC from the SiC substrate, S1 and S2 from the buffer layer, and G from graphene. We adopted a conventional layer-attenuation model using the G/SiC intensity ratio to evaluate the thickness of graphene.<sup>10</sup> For the C 1s peak, the inset in Fig. 2 (a) shows the evolution of the intensity of G-component and that of the ratio S1/S2 with varying  $T_a$ . We find no changes in either the binding energies of the four components or the intensity ratios G/SiC and S1/S2 when Fe are adsorbed on SLG at room temperature (RT), an indicative of no or negligible intercalation of Fe atoms at RT. But these intensity ratios begin to change upon annealing over  $T_a=300$  °C and reach the maximum at  $T_a=600$  °C. For  $T_a > 300$  °C, we notice another component, SiC', appearing with its binding energy shifted by 0.80 eV toward the lower energy side. We ascribe the SiC' to the contribution from carbon atoms in the SiC substrate with a modified dipole layer by the Fe-intercalation<sup>12,31</sup>, since similar shifts have been reported also as 0.7 eV and 2.0 eV by H-<sup>12</sup> and Li-intercalation<sup>13</sup>, respectively. Because the ratio S1/S2 becomes the minimum with the completion of Fe-intercalation at 600 °C, the components S1 and S2 may be safely attributed to the carbon atoms in the buffer layer bonded ( $sp^3$ ) and non-bonded ( $sp^2$ ) to Si atoms of the substrate, respectively. We

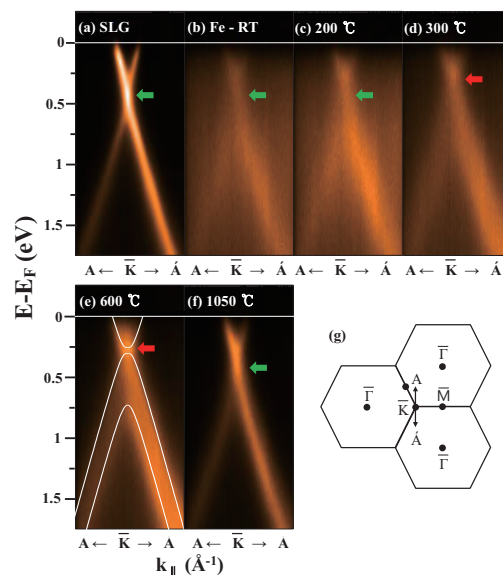


**Fig. 3** Changes of the  $\pi$ -band of the Fe-adsorbed SLG with increasing  $T_a$ . From (a) clean SLG, (b) Fe-adsorbed SLG at RT, and (c)-(f) after annealing at  $200$  °C  $\leq T_a \leq 1050$  °C. Note that the band becomes initially diffused with the adsorption of Fe adatoms, but sharpens again with increasing  $T_a$  showing the split  $\pi$ -bands at  $T_a=600$  °C with a nonuniform distribution of intensity inside. One also notes the Fe-intercalation by the change in Dirac point (red arrow). The white curves in (e) are calculated TB bands from a clean bilayer graphene for comparison. (g) Schematic drawing of the 2D Brillouin zone of graphene

notice that the three components of Si 2p peak, SiC from the substrate, S1 from Si atoms coupled to carbons in the buffer layer, and D from Si defects, remain nearly intact upon annealing below  $T_a=300$  °C. But the evolution of Si 2p with increasing  $T_a$  appears to be quite similar to that of C 1s showing two extra components, SiC' from the substrate SiC as for C 1s, and S1' from the Si atoms directly bonded with Fe atoms, which reach maximum at  $T_a=600$  °C. Annealing above  $T_a=1050$  °C restores its unique core levels for both C 1s and Si 2p before Fe adsorption. We thus conclude that Fe atoms are maximally intercalated below the buffer layer at  $T_a=600$  °C, which results in the decoupling of the buffer layer from its SiC substrate into another quasi free-standing graphene layer as suggested theoretically in Fig. 1(d).

Further and more convincing evidence of Fe-intercalation is found from the changes in the linear  $\pi$ -bands around the  $\bar{K}$  of the graphene Brillouin zone upon annealing above 300 °C. As shown in Fig. 3, the well-defined linear  $\pi$ -band from SLG [Fig. 3 (a)] with the Dirac point  $\sim 0.45$  eV below the Fermi level by the n-doping from the substrate becomes diffused with Fe randomly adsorbed on SLG [Fig. 3 (b)]. With increas-

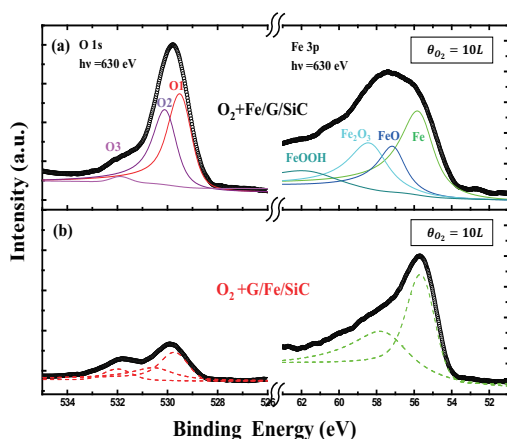


**Fig. 4** Change of O 1s and Fe 3p peaks after exposing 10 L of oxygen to (a) Fe-adsorbed SLG and (b) Fe-intercalated bilayer graphene (BLG/Fe). The HRPES spectra were obtained by using synchrotron photons of energy 630 eV.

ing  $T_a$ , the band becomes fuzzier and broadened [Fig. 3(c) and (d)] before showing two diffused split linear bands best developed with the completion of Fe-intercalation at  $T_a=600$  °C as shown in Fig. 3(d) apparently from the two graphene layers induced by Fe-intercalation. Here unlike the sharp two split bands from clean bilayer graphene, we observe much diffused and broadened split bands with its Dirac point at 0.25 eV below the Fermi level due to the p-doping effect by saturating Si dangling bonds of the buffer layer with Fe atoms. In order to understand the origin of the diffused nature of the Dirac bands, we have carried out DFT band calculations to be discussed below.

Another feature we notice from the Fe-intercalated graphene is the oxidation-retarding effect demonstrated in Fig. 4, where changes of O 1s and Fe 3p core levels are shown after exposing the sample to oxygen environment for (a) Fe-adsorbed SLG (Fe/SLG; top panel) and (b) Fe-intercalated bilayer graphene (BLG/Fe; bottom panel). After exposing to oxygen about 10 Langmuirs (1L= $1 \times 10^{-6}$  Torr sec), we find quite a strong O 1s peak for the Fe/SLG system, while much reduced on the BLG/Fe system from the residual Fe atoms on graphene. Such a difference illustrates so-called a "capping effect" of the bilayer graphene protecting the intercalated Fe atoms from oxidation. This capping effect becomes more pronounced in Fe 3p peak, almost unaffected by oxygen for the BLG/Fe but heavily oxidized for the Fe/SLG. These peaks were fitted with components already reported.<sup>32</sup>

Now we present our DFT-based calculated band structures in Fig. 5 to understand the diffused nature of our spin-integrated Dirac bands observed. Open circles are for the non-spin polarized, and filled circles are for the spin polarized DFT

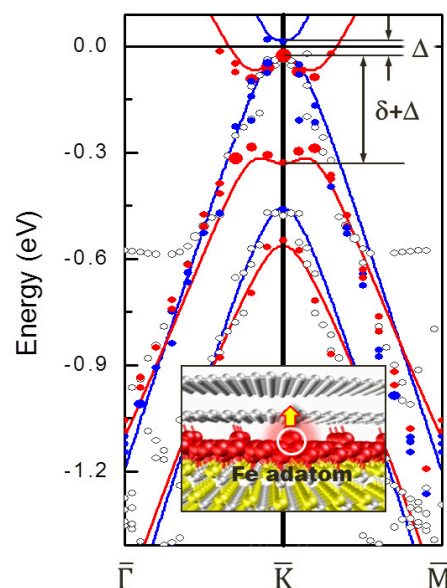


**Fig. 5** DFT-based calculated bands for the Fe-intercalated graphene on SiC(0001). Open, filled red, and filled blue circles are for the spin-integrated, spin-split majority, and minority band, respectively. The red (blue) solid curves are for the majority (minority) spin band using a spin-dependent  $8 \times 8$  tight binding model. Inset shows the side view of the atomic arrangement of the Fe-intercalated layer used for the calculation to emphasize the presence of Fe adatoms.

bands (red for majority and blue for minority). We have assumed a  $4 \times 4$  graphene with some Fe adatoms residing above a single Fe monolayer intercalated below the buffer layer (see the inset). In order to estimate any change in interaction energies from Fe-intercalation such as onsite Coulomb potential  $\Delta$ , spin-dependent exchange energy  $\delta$  between graphene and Fe adatom,<sup>18,33,34</sup> intra- and inter-layer hopping energy  $\gamma_{0i}$  ( $i=1, 2$  for the lower and upper graphene layer, respectively), we have also adopted an  $8 \times 8$  spin polarized tight-binding (TB) model. The solid curves in Fig. 5 denote the TB bands from this model, which are to be compared with the DFT bands. Here we note two different values of  $\delta_A$  and  $\delta_B$  for the two sublattices A and B of graphene due to the different degree of hybridization of Fe adatom with the buffer layer other than the spin-dependent exchange energy.

From these bands in Fig. 5, we first notice a distinct energy gap of  $\Delta + \delta = 0.30$  eV for the majority spin band while quite a small gap  $\Delta \leq 0.05$  eV for the minority band. This small gap  $\Delta$  essentially suggests only a slight difference in charge distribution between the graphene layers since it arises mainly from the on-site Coulomb potential. As depicted in the inset of Fig. 5, we have a bilayer graphene system with partially spin-injected C atoms existing only in the lower graphene through the exchange proximity effect. These spin-

injected C atoms appear to have the same spin character with Fe adatoms, while atoms in the upper graphene remain nearly intact with Fe-intercalation having almost no magnetic moment. More specifically the spin-injected C atoms near Fe adatom in the lower graphene have the magnetic moment about  $0.007\sim 0.010 \mu_B$  while those in the upper graphene have smaller than  $0.001 \mu_B$ . This asymmetry in spin between the upper and lower graphene layers primarily modifies  $\delta$ , which turns out to be the driving force for the spin-polarized paired bands shown in Fig. 5. Apparently such a change also disturbs the nearest hopping energy  $\gamma_1$  in the lower graphene of majority spin so that electrons of different spins should show different mobilities as demonstrated by the crossing between the majority (red) and minority (blue curves) TB bands in Fig. 5.

Using  $\gamma_0=2.8$  eV for both majority and minority spins and  $\gamma_1=0.40$  (0.45) eV for majority (minority) spin in the  $8\times 8$  TB model,<sup>33</sup> we have fitted our measured bands in Fig. 3 (e) to determine these coupling energies for the Fe-intercalated graphene system. From the best fit, we obtain  $\Delta=0.05$  eV,  $\delta_A=0.25$  eV, and  $\delta_B=0.35$  eV for the majority bands of the lower graphene, which are significant values for  $\delta$  in comparison with the vanishing one for the minority band or the bands in the upper graphene layer. Such a non-vanishing  $\delta$  clearly shows the presence of spin-injected carbon atoms only in the lower graphene and its exchange proximity effect. We also find the reduced  $\gamma_1=2.0$  eV due to the spin effect from its initial value 2.8 eV of the pristine graphene. The much enhanced exchange energy  $\delta \geq 5\Delta$  for the lower graphene in sharp contrast with the vanishing  $\delta$  for the upper graphene illustrates the significant spin asymmetry between the graphene layers, which drives the formation of multiple spin-split bands centered at  $\bar{K}$  as presented in Fig. 5. These spin-split multiple bands diffused by thermal broadening at room temperature become closely jammed near  $\bar{K}$ , and thus may appear fuzzy as observed in Fig. 3 (e). Since these spin-dependent interaction energies can be controlled rather easily by varying Fe-coverage, one may be able to design or tune the spin-polarized band structures of spin-injected Fe-graphene system for industrial application.

#### 4 Summary and Conclusions

In summary, we have studied intercalation of Fe adatoms on SLG formed on the SiC(0001) surface especially focussed on any change in electronic and structural properties induced by the spin of intercalated Fe atoms. Our data of both linear  $\pi$ -bands and C 1s, Si 2p, and Fe 3p surface core levels modified by Fe-doping unambiguously reveal evidence for the intercalation of Fe atoms below the buffer layer forming two weakly coupled bilayer graphene. The split  $\pi$ -bands measured from the Fe-intercalated bilayer graphene, however, appear to be much diffused and fuzzy. Since our DFT- as well as TB-based

calculations for this system exhibit the presence of multiple spin-polarized  $\pi$ -bands, we ascribe such diffused nature of the measured bands to these co-existing spin-split bands. By fitting our theoretical  $\pi$ -bands with the measured data, we estimate the interaction energies ( $\Delta$ ,  $\delta$ , and  $\gamma_0$ ) associated with the intercalated Fe atoms. We notice a distinct symmetry breaking not only in charge and spin distributions but also in these interaction energies between the two graphene layers. Such distinct asymmetries stem essentially from the spin-injected carbon atoms in the lower graphene, a noble feature not ever seen from the intercalation of non-magnetic atoms through graphene, which may have a significant potential application on future graphene-based spintronics devices.

#### Acknowledgments

This work was supported by the National Research Foundation of Korea(NRF) grant funded by the Korea government(MSIP) (2008-0062606, CELA-NCRC), by the Ministry of Science, ICT and Future Planning (NRF-2013R1A1A2005598), and also in part by the Steel Science Program funded by POSCO (4.0004556.01). KSK acknowledges support by National Honor Scientist Program: 2010-0020414, WCU, CCH by the SRC Center for Topological Matter: 2011-0030787, and JSK by the POSTECH Basic Science Research Institute Grant 4.0008000.01.

#### References

- 1 K. S. Novoselov, A. K. Geim, S. V. Morozov, D. Jiang, Y. Zhang, S. V. Dubonos, I. V. Grigorieva and A. A. Firsov, *Science*, 2004, **306**, 666–669.
- 2 K. S. Novoselov, A. K. Geim, S. V. Morozov, D. Jiang, M. I. Katsnelson, I. V. Grigorieva, S. V. Dubonos and A. A. Firsov, *Nature*, 2005, **438**, 197–200.
- 3 Y. Zhang, Y. Tan, H. Stormer and P. Kim, *Nature*, 2005, **438**, 201.
- 4 W. Y. Kim and K. S. Kim, *Nature Nanotech.*, 2008, **3**, 408–412.
- 5 K. S. Kim, Y. Zhao, H. Jang, S. Y. Lee, J. M. Kim, K. S. Kim, J. H. Ahn, P. Kim, J. Y. Choi and B. H. Hong., *Nature*, 2009, **457**, 706–710.
- 6 S. Bae, H. Kim, Y. Lee, X. Xu, J.-S. Park, Y. Zheng, J. Balakrishnan, T. Lei, H. R. Kim, Y. I. Song, Y.-J. Kim, K. S. Kim, B. Ozyilmaz, J.-H. Ahn, B. H. Hong and S. Iijima., *Nature Nanotech.*, 2010, **5**, 574–578.
- 7 C. Berger, Z. Song, X. Li, X. Wu, N. Brown, C. Naud, D. Mayou, T. Li, J. Hass, A. N. Marchenkov, E. H. Conrad, P. N. First and W. A. de Heer, *Science*, 2006, **312**, 1191–1196.
- 8 T. Ohta, A. Bostwick, T. Seyller, K. Horn and E. Rotenberg, *Science*, 2006, **313**, 951–954.
- 9 C. Berger, X. Wu, P. N. First, E. H. Conrad, X. Li, M. Sprinkle, J. Hass, F. Varchon, L. Magaud, M. L. Sadowski, M. Potemski, G. Martinez and W. A. de Heer, *Adv. Solid State Phys.*, 2008, **47**, 145–157.

<sup>a</sup> Department of Physics, Pohang University of Science and Technology, Pohang, Korea. Fax: +82-54-279-3099; Tel: +82-54-279-2071; E-mail: jwc@postech.ac.kr

<sup>b</sup> Beamline Research Division, Pohang Accelerator Laboratory, Pohang, Korea.

<sup>c</sup> Department of Chemistry, Pohang University of Science and Technology, Pohang, Korea.

- 10 K. V. Emtsev, F. Speck, T. Seyller and L. Ley., *Phys. Rev. B.*, 2009, **77**, 155303.
- 11 A. Mattausch and O. Pankratov, *Phys. Rev. Lett.*, 2007, **99**, 076802.
- 12 C. Riedl, C. Coletti, T. Iwasaki, A. A. Zakharov and U. Starke, *Phys. Rev. Lett.*, 2009, **103**, 246804.
- 13 C. Virojanadara, S. Watcharinyanon, A. A. Zakharov and L. I. Johansson, *Phys. Rev. B.*, 2010, **82**, 205402.
- 14 I. Gierz, T. Suzuki, T. Weitz, D. S. Lee, B. Krauss, C. Riedl, U. Starke, H. Hchst, J. H. Smet, C. R. Ast and K. Kern, *Phys. Rev. B.*, 2010, **81**, 235408.
- 15 S. Oida, F. R. McFeely, J. B. Hannon, R. M. Tromp, M. Copel, Z. Chen, Y. Sun, D. B. Farmer and J. Yurkas, *Phys. Rev. B.*, 2010, **82**, 041411.
- 16 K. V. Emtsev, A. A. Zakharov, C. Coletti, S. Forti and U. Starke, *Phys. Rev. B.*, 2011, **84**, 125423.
- 17 C. Xia, S. Watcharinyanon, A. A. Zakharov, R. Yakimova, L. Hultman, L. I. Johansson and C. Virojanadara, *Phys. Rev. B.*, 2012, **85**, 045418.
- 18 H. X. Yang, A. Hallal, D. Terrade, X. Waintal, S. Roche and M. Chshiev, *Phys. Rev. Lett.*, 2013, **110**, 046603.
- 19 N. Tombros, C. Jozsa, M. Popinciuc, H. T. Jonkman and B. J. van Wees, *Nature*, 2007, **448**, 571.
- 20 M. Weser, Y. Rehder, K. Horn, M. Sicot, M. Fonin, A. B. Preobrajenski, E. N. Voloshina, E. Goering and Y. S. Dedkov, *Appl. Phys. Lett.*, 2010, **96**, 012504.
- 21 Y. S. Dedkov and M. Fonin, *New J. Phys.*, 2010, **12**, 125004.
- 22 J. Coraux, A. T. NDiaye, N. Rougemaille, C. Vo-Van, A. Kimouche, H.-X. Yang, M. Chshiev, N. Bendiab, O. Fruchart and A. K. Schmid, *J. Phys. Chem. Lett.*, 2012, **3**, 2059–2063.
- 23 C. G. Hwang, S. Y. Shin, S.-M. Choi, N. D. Kim, S. H. Uhm, H. S. Kim, C. C. Hwang, D. Y. Noh, S.-H. Jhi and J. W. Chung, *Phys. Rev. B.*, 2009, **79**, 115439.
- 24 S. Y. Shin, C. G. Hwang, S. J. Sung, N. D. Kim, H. S. Kim and J. W. Chung, *Phys. Rev. B (Rapid Commun.)*, 2011, **83**, 161403(R).
- 25 G. Kresse and J. Furthmüller, *Phys. Rev. B.*, 1996, **54**, 11169.
- 26 Neugebauer and Scheffler, *Phys. Rev. B.*, 1992, **46**, 16067.
- 27 G. Kresse and D. Joubert, *Phys. Rev. B.*, 1999, **59**, 1758.
- 28 J. Klimes, D. R. Bowler and A. Michaelides, *Phys. Rev. B.*, 2011, **83**, 195131.
- 29 L. I. Johansson, F. Owman and P. Martensson, *Phys. Rev. B.*, 1996, **53**, 13793.
- 30 P. H. Mahowald, D. J. Friedman, G. P. Carey, K. A. Bertness and J. J. Yeah, *Vac. Sci. Technol. A.*, 1987, **5**, 2982.
- 31 S. Watcharinyanon, C. Virojanadara, J. Osiecki, A. Zakharov, R. Yakimova, R. Uhrberg and L. Johansson, *Surf. Sci.*, 2011, **605**, 1662.
- 32 L. P. Kazansky., Y. I. Kuznetsov., N. P. Andreeva and Y. G. Bober, *Surf. Sci.*, 2010, **257**, 11166.
- 33 W. W. Toy, M. S. Dresselhaus and G. Dresselhaus, *Phys. Rev. B.*, 1977, **15**, 4077.
- 34 E. McCann, *Phys. Rev. B.*, 2006, **74**, 161403.

## The table of contents entry

Fe adatoms are intercalated through epitaxial graphene to form a bilayer graphene, which shows spin-polarized Dirac bands arising from spin-injected C atoms.

